Linear stability of a circular Couette flow under a radial thermoelectric body force

H. N. Yoshikawa,* A. Meyer, O. Crumeyrolle, and I. Mutabazi
Laboratoire Ondes et Milieux Complexes, UMR 6294 CNRS-Université du Havre, 53, rue de Prony-76058 Le Havre Cedex, France
(Received 23 December 2014; published 3 March 2015)

The stability of the circular Couette flow of a dielectric fluid is analyzed by a linear perturbation theory. The fluid is confined between two concentric cylindrical electrodes of infinite length with only the inner one rotating. A temperature difference and an alternating electric tension are applied to the electrodes to produce a radial dielectrophoretic body force that can induce convection in the fluid. We examine the effects of superposition of this thermoelectric force with the centrifugal force including its thermal variation. The Earth's gravity is neglected to focus on the situations of a vanishing Grashof number such as microgravity conditions. Depending on the electric field strength and of the temperature difference, critical modes are either axisymmetric or nonaxisymmetric, occurring in either stationary or oscillatory states. An energetic analysis is performed to determine the dominant destabilizing mechanism. When the inner cylinder is hotter than the outer one, the circular Couette flow is destabilized by the centrifugal force for weak and moderate electric fields. The critical mode is steady axisymmetric, except for weak fields within a certain range of the Prandtl number and of the radius ratio of the cylinders, where the mode is oscillatory and axisymmetric. The frequency of this oscillatory mode is correlated with a Brunt-Väisälä frequency due to the stratification of both the density and the electric permittivity of the fluid. Under strong electric fields, the destabilization by the dielectrophoretic force is dominant, leading to oscillatory nonaxisymmetric critical modes with a frequency scaled by the frequency of the inner-cylinder rotation. When the outer cylinder is hotter than the inner one, the instability is again driven by the centrifugal force. The critical mode is axisymmetric and either steady under weak electric fields or oscillatory under strong electric fields. The frequency of the oscillatory mode is also correlated with the Brunt-Väisälä frequency.

DOI: 10.1103/PhysRevE.91.033003 PACS number(s): 47.20.Qr, 44.27.+g

I. INTRODUCTION

The Taylor-Couette flow is a prototype system in nonlinear physics and it exhibits a rich variety of bifurcation phenomena (see, e.g., Refs. [1,2]). This flow and its variants are encountered in many applications, concerning the mass, heat, and momentum transfer in rotating machinery and in process industries. Geophysical flows in the atmosphere of rapidly rotating major planets have also been modelled as Taylor-Couette flows, by dividing the spherical shell of a planet into superimposed coaxial annular layers [3–5].

In diverse applications, the temperature of the fluid in differentially rotating cylindrical annuli is not uniform. This nonuniformity can induce drastic effects on flow regimes. Effects of a radial temperature gradient on the centrifugal instability have been examined experimentally [6–9]. Convection rolls inclined with respect to the azimuthal direction have been observed when the temperature difference was significant. Controversial results have been reported with regard to the effects of the heating direction: some observed its influence on the stability; others did not. Although stability analyses have also been performed [10–13], they often neglected the thermal variation of the centrifugal force. Recently, Yoshikawa *et al.* [14] revisited the problem and confirmed that the stability is sensitive to the heating direction when the thermal variation of centrifugal force is significant: the flow is more stable under an outward heating (i.e., the inner cylinder is hotter than the outer one) than under inward heating (i.e., the outer cylinder is hotter than the inner one). This result can be explained by the fact that the density stratification is stable (potentially unstable) in the centrifugal acceleration field under outward (inward) heating.

The dependence of the stability on the heating direction can also result from other radial thermal body forces than the centrifugal force. Tagg and Weidman [15] considered a magnetic fluid in a vertical Taylor-Couette system with only the inner cylinder rotating. The thermal variation of the magnetization leads to a thermomagnetic body force density, which can be viewed as a thermal buoyancy force associated with a radial magnetic effective gravity. The authors analyzed the linear stability of a base flow driven both by the inner cylinder rotation and by the differential heating under the Earth's gravity and examined the behavior of the critical flow parameters as a function of the Grashof number. It was found that outward heating destabilized the flow significantly when the magnetic body force was of the same order of magnitude as the Earth's gravity force. When the heating direction was inverted, the thermomagnetic force yielded an important stabilizing effect.

Another means to produce a radial thermal body force is an alternating radial electric field. The application of an electric field $\boldsymbol{E}$ to a dielectric fluid results in the *electrohydrodynamic (EHD)* body force. Its density $\mathbf{f}$ is given by

$$\mathbf{f} = \rho_e \boldsymbol{E} - \frac{1}{2} E^2 \nabla \epsilon + \nabla \left[\frac{1}{2} \rho \left(\frac{\partial \epsilon}{\partial \rho} \right)_T E^2 \right], \qquad (1)$$

where ρ_e is the free charge density, E is the strength of the electric field ($E = |\boldsymbol{E}|$), and ρ and ϵ are, respectively, the density and the electric permittivity of the fluid at the local temperature T [17,18]. The first term, called *the electrophoretic force*, reflects the Coulomb forces on the free

*Present address: Laboratoire J.-A. Dieudonné, UMR 7351 CNRS-Université Nice Sophia Antipolis, Parc Valrose - 06108, Nice Cedex 02, France; Email: harunori@unice.fr

charges. The second term, called *the dielectrophoretic (DEP) force*, arises from the differential polarization of the fluid. The third term represents electrostriction, which can be lumped with the pressure in the momentum equation and would not affect the fluid motion, unless the fluid is compressible or has mobile boundaries. When the electric field is static or alternating with a low frequency, the electrophoretic force has dominant effects on the fluid motion. However, when the frequency f of the field is high compared to the inverse of the fluid relaxation times $\tau_\nu = d^2/\nu$ and $\tau_\kappa = d^2/\kappa$ (d, the characteristic length scale of the flow; ν and κ, the kinematic viscosity and the thermal diffusivity of the fluid, respectively), the electrophoretic force is filtered out by viscous and thermal relaxation and the DEP force becomes dominant.

The DEP force can arise from a temperature gradient in fluid, as the permittivity varies with the temperature. Its variation can be modelled by a linear relationship $\epsilon = \epsilon_{\text{ref}}\,[1 - e\,(T - T_{\text{ref}})]$, where ϵ_{ref} is the permittivity at reference temperature T_{ref}. The coefficient e takes a positive value of the order of 10^{-3}–10^{-1} K^{-1} (e.g., Table I). Substituting ϵ by the linear relationship, the DEP force can be written as

$$-\frac{1}{2}E^2\nabla\epsilon = -e\theta\nabla\frac{\epsilon_{\text{ref}}E^2}{2} + \nabla\left(\frac{e\theta\epsilon_{\text{ref}}E^2}{2}\right), \qquad (2)$$

where θ is the temperature deviation: $\theta = T - T_{\text{ref}}$. Casting the first term into the form of $-\alpha\theta\boldsymbol{g}_e$, we can regard it as thermal buoyancy associated with an electric effective gravity $\boldsymbol{g}_e$ [19–21]:

$$\boldsymbol{g}_e = \frac{e}{\alpha\rho}\nabla\frac{\epsilon_{\text{ref}}E^2}{2}, \qquad (3)$$

where α is the coefficient of thermal expansion. The second term in Eq. (2) can be lumped with the pressure term in the momentum equation. In analogy with the thermal Archimedean buoyancy, the thermoelectric buoyancy ($-\alpha\theta\boldsymbol{g}_e$) will induce a thermal convection when the following Rayleigh number L based on g_e ($= |\boldsymbol{g}_e|$) becomes larger than a critical value L_c:

$$L = \frac{\alpha\Delta\theta g_e d^3}{\nu\kappa}. \qquad (4)$$

Here, $\Delta\theta$ is the temperature difference in the fluid. When a radial electric field is applied to a fluid in a cylindrical annulus, the electric gravity $\boldsymbol{g}_e$ and associated thermoelectric buoyancy are directed radially.

The analogy of the thermomagnetic or thermoelectric buoyancy forces with the thermal Archimedean buoyancy is of great interest in geo- and astrophysics, where convective flows and stratified shear flows in the central gravity field are of primary importance. Realization of laboratory experiments with an artificial radial gravity is a key to advance the understanding of these flows. Some attempts have been made with the thermoelectric artificial gravity in annular geometry [20,22,23] and in spherical geometry [24–28]. An experiment with the thermomagnetic artificial gravity has also been reported in annular geometry [29].

Theoretical investigations on the thermal convection in the electric gravity have been carried out in different capacitor geometries under microgravity conditions. In the annular geometry with stationary cylinders, Chandra and Smylie [20] and Takashima [30] examined the stability of the conductive state against axisymmetric disturbances. The considered geometries were small gap annuli: the ratio η of inner to outer cylinder radii was larger than 0.9. Recently, Malik *et al.* [31] and Yoshikawa *et al.* [21] performed linear stability analyses for annuli with arbitrary gap and for arbitrary perturbations. Their analyses showed that the critical mode is a steady spiral. Treating both inward and outward heating, the latter authors investigated exhaustively the effects of the radius ratio η and the thermoelectric parameter $\gamma_e = e\Delta\theta$. The direction of the electric gravity was shown to depend on these two parameters and can be centripetal, centrifugal, *or* centripetal in an inner layer and centrifugal in the outer layer. Instability can occur only either in outward heating where the electric gravity is centripetal *or* in inward heating when the electric gravity is centrifugal. The authors performed an energetic analysis and showed that the temperature disturbances induce a perturbation component $\boldsymbol{g}'_e$ of the electric gravity, which plays a key role in the stabilization of the flow for large values of the radius ratio. This stabilizing effect has also been observed in the analysis on the thermoelectric convection in the plane geometry [32] and explained its quantitative differences from the Rayleigh-Bénard convection in critical flow parameters as well as in the heat transfer by developed convective flows.

The circular Couette flow with the inner cylinder rotating and under the action of thermoelectric body force has been considered by Stiles and Kagan [33]. Their study was focused on axisymmetric steady perturbations in a small gap geometry. Only outward heating was considered. They obtained steady critical modes and found that the critical Taylor number dropped effectively with the temperature difference.

In the present paper, we report a linear stability analysis of the circular Couette flow to arbitrary perturbations when

TABLE I. Properties of some dielectric liquids.

Liquid	ν (10^{-6} m^2/s)	ρ (kg/m^3)	α (10^{-3} K^{-1})	ϵ_r	e (10^{-3} K^{-1})	Pr	α/e
Acetonitrile	0.439	777	1.38	36.0	155	4.7	0.00890
Nitrobenzene	1.52	1198	0.83	34.9	188	19	0.00441
Acetone	0.386	785	1.43	19.1	86	4.2	0.0166
Chlorobenzene	0.686	1101	0.985	5.61	15.7	7.9	0.0627
Cyclohexane	1.17	774	1.22	2.02	1.60	14	0.763
Silicone oil[a]	5.0	920	1.08	2.70	1.065	59.9	1.01
Silicone oil[b]	99.2	968	0.96	2.73	3.2	910	0.3

[a]Baysilone M5.
[b]After the properties given in Ref. [16].

the flow is under the thermoelectric body force. Both inward and outward heatings are considered. The analysis focuses on the centripetal configuration of the electric gravity, i.e., the case that is the most relevant to the application in geo- and astrophysics, while some results will also be given for the other configurations (Sec. V C). Effects of the thermal variation of the centrifugal force on the stability are examined with varying the thermal expansion parameter $\gamma_a = \alpha\Delta\theta$. We will show that, depending on flow parameters, critical states occur either steady or oscillatory and as either axisymmetric or nonaxisymmetric modes.

In Sec. II, a mathematical model is presented with the conductive base state. Section III is devoted to the formulation of the linear stability problem. Critical values of flow parameters and corresponding critical states will be described in Sec. IV: first for a particular case of $\gamma_a = 0$ and then for more general cases with nonzero γ_a. The variation of the critical parameters with the radius ratio and the Prandtl number is considered. Eigenfunctions of different states are presented. Section V is devoted to analysis of the critical modes: a focus is made on the energy transfer process to critical modes in different states and on the origin of the critical frequencies. Section VI gives our concluding remarks.

II. MATHEMATICAL MODEL

We consider a Taylor-Couette system that confines a dielectric fluid in the gap d between two concentric cylindrical electrodes of infinite length (Fig. 1). The radii of the inner and outer electrodes are R_1 and R_2 $(= R_1 + d)$, respectively. The inner cylinder rotates at angular velocity Ω and it is kept at temperature T_1, while the outer one is at rest and it is maintained at temperature T_2. The annulus is subjected to both a temperature difference $\Delta\theta = T_1 - T_2$ and an alternating electric tension $\sqrt{2}\Phi_0 \sin(2\pi f t)$. The flow is under the action of the centrifugal force due to the cylinder rotation and the thermoelectric body force due to the electric gravity [Eq. (3)].

A. Governing equations

We have adopted the electrohydrodynamic Boussinesq approximation [34], which consists in keeping the fluid properties independent of temperature, except in the terms that are responsible for instability mechanisms. These are the centrifugal force and the dielectrophoretic force. The governing equations are the conservation laws of the mass, the momentum, and the energy and the Gauss' law for electricity; they can be written as follows:

$$\nabla \cdot \boldsymbol{u} = 0, \tag{5}$$

$$\frac{\partial \boldsymbol{u}}{\partial t} + \boldsymbol{u} \cdot \nabla \boldsymbol{u} = -\nabla \pi + \nu \nabla^2 \boldsymbol{u} - \alpha\theta\,(\boldsymbol{g}_e + \boldsymbol{g}_c), \tag{6}$$

$$\frac{\partial \theta}{\partial t} + \boldsymbol{u} \cdot \nabla \theta = \kappa \nabla^2 \theta, \tag{7}$$

$$\nabla \cdot (\epsilon \boldsymbol{E}) = 0 \quad \text{with} \quad \epsilon = \epsilon_2 (1 - e\theta) \quad \text{and} \quad \boldsymbol{E} = -\nabla\phi, \tag{8}$$

where the electrostatic potential ϕ and the following generalized hydrodynamic pressure π have been introduced:

$$\pi = \frac{p}{\rho} - \frac{e\theta\epsilon_{\text{ref}} E^2}{2\rho} - \frac{1}{2}\left(\frac{\partial \epsilon}{\partial \rho}\right)_T E^2. \tag{9}$$

The reference temperature is set at T_2 so that $\theta = T - T_2$ and $\epsilon_{\text{ref}} = \epsilon_2$. The last term of the Navier-Stokes Eq. (6) represents two thermal buoyancies: one from the electric gravity and the other from the centrifugal acceleration $\boldsymbol{g}_c$ given by

$$\boldsymbol{g}_c = \frac{v^2}{r}\boldsymbol{e}_r, \tag{10}$$

where v is the azimuthal velocity and $\boldsymbol{e}_r$ is the radial unit vector. We call the term $(-\alpha\theta\boldsymbol{g}_c)$ *the centrifugal buoyancy* in order to emphasize its origin in the centrifugal force, although it can be either centrifugal or centripetal depending on the heating direction.

We have assumed the electroneutrality of the fluid in Eq. (8). This assumption is valid when the frequency f of the applied electric field is high enough to neglect the motion of free charges in the fluid during a period f^{-1} and when the size of the fluid system is large compared to the electric double layer on the electrodes [32].

We have also assumed that $f \gg \tau_v^{-1}, \tau_\kappa^{-1}$ for the dominance of the DEP force over the electrophoretic force. Under this assumption, only the time-averaged component of the thermoelectric buoyancy can affect the fluid motion and we can reduce the problem with an a.c. electric field to an equivalent problem with an effective static field. In this time-averaged description, the boundary conditions on the electrodes read

$$\boldsymbol{u} = R_1\Omega\boldsymbol{e}_\varphi, \quad \theta = \Delta\theta, \quad \phi = \Phi_0 \quad \text{at } r = R_1, \tag{11}$$

$$\boldsymbol{u} = 0, \quad \theta = 0, \quad \phi = 0 \quad \text{at } r = R_2. \tag{12}$$

The time-averaged description was found to predict successfully the behavior of dielectric fluids in experiments [35]. A theoretical investigation on the influence of the frequency suggests that the description is correct when $2\pi f \gtrsim 100\ \tau_v^{-1}$ [36]. This condition was met in an experiment performed in annular geometry [22] with a silicone oil of viscosity $\nu = 10\ \text{mm}^2/\text{s}$. For the gap width $d = 25$ mm and the frequency of applied electric tension $f = 50$ Hz, the viscous relaxation time is $\tau_v = 62.5$ s so that $f \gg 100\tau_v^{-1} = 1.6$ Hz.

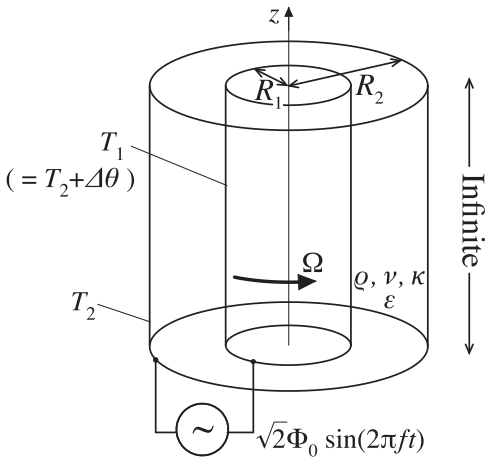

FIG. 1. Geometrical configuration of the problem.

B. Base state

For a small temperature difference and a small rotation velocity, the state of the system will respect its symmetry in time and in space. The velocity $\boldsymbol{U}$, the temperature Θ, and the electric potential Φ are stationary and depend only on the radial coordinate r: $\boldsymbol{U} = V(r)\boldsymbol{e}_\varphi$, $\Theta = \Theta(r)$, and $\Phi = \Phi(r)$. The advective transport vanishes ($\boldsymbol{u}\cdot\boldsymbol{\nabla} = 0$) so that the base state has the velocity profile of a circular Couette flow and the temperature and the electric fields are decoupled from the flow velocity. From Eqs.(6)–(12), one finds

$$\boldsymbol{U}(r) = V(r)\boldsymbol{e}_\varphi \quad \text{with} \quad V(r) = \frac{\Omega}{1-\eta^2}\left(\frac{R_1^2}{r} - \eta^2 r\right), \tag{13}$$

$$\Theta(r) = \frac{\Delta\theta \log(r/R_2)}{\log\eta}, \quad \Phi(r) = \frac{\Phi_0 \log(1-\gamma_e\Theta/\Delta\theta)}{\log(1-\gamma_e)}, \tag{14}$$

where $\eta = R_1/R_2$. The corresponding electric gravity is [21]

$$\boldsymbol{G}_e = -G_e\boldsymbol{e}_r, \quad \text{with}$$

$$G_e = \frac{e\epsilon_2\Phi_0^2}{\alpha\rho(\log\eta)^2 r^3}\cdot\frac{\gamma_e^2[1-\gamma_e(\Theta/\Delta\theta + 1/\log\eta)]}{[\log(1-\gamma_e)]^2(1-\gamma_e\Theta/\Delta\theta)^3}. \tag{15}$$

The second factor in the last term modifies an inverse cube law ($G_e \propto 1/r^3$) as a consequence of a competition between the effects of the geometry curvature and the thermal stratification of the electric permittivity. This competition brings a variety of behavior [21]: the electric gravity is centripetal (i.e., $G_e > 0$) when $\gamma_e > \log\eta$; it is centrifugal (i.e., $G_e < 0$) when $\gamma_e < \log\eta/(1+\log\eta)$; it changes the direction inside the gap when $\log\eta/(1+\log\eta) < \gamma_e < \log\eta$.

III. STABILITY ANALYSIS

We consider the stability of the base state Eqs. (13)–(14) against arbitrary infinitesimal perturbations $(u',v',w',\pi',\theta',\phi')$, where (u',v',w') are the radial, azimuthal, and axial components of the perturbation velocity, θ' is the perturbation temperature, π' is the perturbation pressure, and ϕ' is the perturbation electrostatic potential. We linearize the governing Eqs. (5)–(8), and expand the perturbations into normal modes: $(u',v',w',\pi',\theta',\phi') = (\tilde{u},\tilde{v},\tilde{w},\tilde{\pi},\tilde{\theta},\tilde{\phi})\ \exp[st + in\varphi + ikz]$. A tilde over a quantity indicates its complex amplitude. The perturbation growth rate s may be complex: $s = \sigma + i\omega$, where ω is the frequency of the mode. The axial wavenumber k is a real number, as the perturbations are bounded at infinity. The azimuthal mode number n takes only integer values.

Introducing the scales d of length, d^2/ν of time, ν/d of velocity, $\Delta\theta$ of temperature, and Φ_0 of electric potential, the linearized governing equations become dimensionless and read

$$\frac{1}{r}D(r\tilde{u}) + \frac{in\tilde{v}}{r} + ik\tilde{w} = 0, \tag{16}$$

$$s\tilde{u} + \frac{inV}{r}\tilde{u} = -D\tilde{\pi} + \nabla^2\tilde{u} - \frac{\tilde{u}}{r^2} + 2\frac{V\tilde{v}}{r} - \frac{2in}{r^2}\tilde{v} - \frac{L}{\mathrm{Pr}}(-G_e\tilde{\theta} + \Theta\tilde{g}_{e,r}) - \frac{\gamma_a}{r}(\tilde{\theta}V^2 + 2\Theta V\tilde{v}), \tag{17}$$

$$s\tilde{v} + \frac{inV}{r}\tilde{v} = -\frac{in}{r}\tilde{\pi} + \nabla^2\tilde{v} - \frac{\tilde{v}}{r^2} - \frac{\tilde{u}V}{r} + \frac{2in}{r^2}\tilde{u} - (DV)\tilde{u} - \frac{L}{\mathrm{Pr}}\Theta\tilde{g}_{e,\varphi}, \tag{18}$$

$$s\tilde{w} + \frac{inV}{r}\tilde{w} = -ik\tilde{\pi} + \nabla^2\tilde{w} - \frac{L}{\mathrm{Pr}}\Theta\tilde{g}_{e,z}, \tag{19}$$

$$s\tilde{\theta} + \frac{inV}{r}\tilde{\theta} = -(D\Theta)\,\tilde{u} + \frac{1}{\mathrm{Pr}}\nabla^2\tilde{\theta}, \tag{20}$$

$$(1-\gamma_e\Theta)\nabla^2\tilde{\phi} - \gamma_e D\Theta D\tilde{\phi} - \gamma_e D\Phi\left(D + \frac{1}{r}\right)\tilde{\theta} - \gamma_e(D^2\Phi)\tilde{\theta} = 0, \tag{21}$$

where $D = d/dr$ and $\nabla^2 = D^2 + \frac{1}{r}D - \frac{n^2}{r^2} - k^2$. The Taylor number Ta and the Prandtl number Pr are defined as:

$$\mathrm{Ta} = \frac{R_1\Omega d}{\nu}\sqrt{\frac{d}{R_1}}, \quad \mathrm{Pr} = \frac{\nu}{\kappa}. \tag{22}$$

In the electric Rayleigh number L defined by Eq.(4), we choose the base electric gravity at the middle of the gap $G_{e,0} = G_e(r_0)$ as representative one, where r_0 is the dimensionless midgap radius: $r_0 = (1+\eta)/2(1-\eta)$. For a centripetal electric gravity field ($G_e > 0$), the Rayleigh number L is positive in outward heating and negative in inward heating. The perturbation electric gravity $(\tilde{g}_{e,r},\tilde{g}_{e,\varphi},\tilde{g}_{e,z})$ is related to the perturbation electric field resulting from temperature disturbances. This perturbation gravity as well as the base gravity have been nondimensionalized with the scale $G_{e,0}$. The explicit expressions of the dimensionless gravities are given in Ref. [21].

The linearized Eqs. (16)–(21) supplemented with the homogeneous boundary conditions $(\tilde{u},\tilde{v},\tilde{w},\tilde{\theta},\tilde{\phi}) = 0$ at the cylinder surfaces form an eigenvalue problem represented formally by

$$\mathcal{F}(s,\mathrm{Ta},L,n,k,\eta,\mathrm{Pr},\gamma_e,\gamma_a) = 0. \tag{23}$$

The Taylor number intervenes in the problem through the base flow V ($\propto$ Ta). To determine the eigenvalue, Eqs. (16)–(21) are discretised by a Chebyshev spectral collocation method and Eq. (23) is transformed into a generalized eigenvalue problem in matrix form. The latter is solved by the QZ decomposition. The highest order of considered Chebyshev polynomials is set from 15 to 28 to ensure the convergence, depending on the radius ratio.

IV. RESULTS

Eigenvalues s of the linear stability problem formulated in Sec. III are computed for a given parameter set $(L,n,\eta,\mathrm{Pr},\gamma_e,\gamma_a)$ at different (k,Ta). A marginal stability curve $\mathrm{Ta} = \mathrm{Ta}(k)$ is determined by seeking the condition that the largest real part σ of s changes its sign. The minimum of a marginal curve gives the instability threshold (k_n,Ta_n) of the azimuthal mode n. The smallest value of $\{\mathrm{Ta}_n\}$ and the corresponding values of (n,k_n,ω_n) give the critical parameters $(\mathrm{Ta},k_c,n_c,\omega_c)$. The critical wavenumber q_c of vortices is computed on the median cylindrical surface $r = r_0$ from the

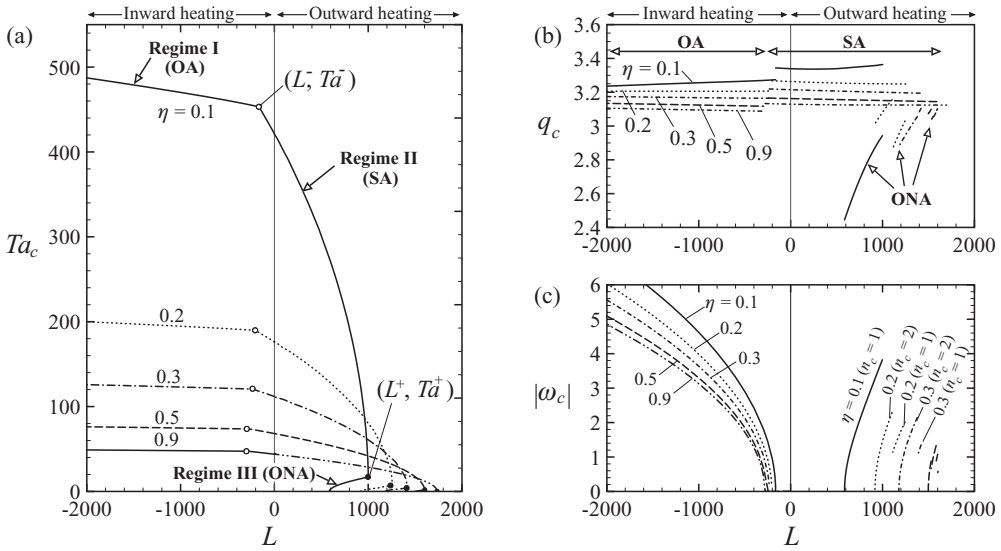

FIG. 2. Critical parameters for different radius ratios η (Pr = 10): Taylor number (a), wavenumber of vortices (b), and frequency (c). The centrifugal buoyancy is neglected ($\gamma_a = 0$). The thermoelectric parameter is fixed at $\gamma_e = -0.01$ and 0.01 for inward and outward heating, respectively. The critical modes are oscillatory axisymmetric (OA), steady axisymmetric (SA), or oscillatory nonaxisymmetric (ONA). In panel (a), the codimension-2 points are indicated by open and filled circles.

pair (k_c, n_c) by $q_c = (k_c^2 + k_{\varphi,c}^2)^{1/2}$, where $k_{\varphi,c} = n_c/r_0$ is the azimuthal wavenumber. We present these critical parameters for different values of L in two cases: a particular case where the centrifugal buoyancy is neglected (i.e., $\gamma_a = 0$) and the general case with the centrifugal buoyancy (i.e., $\gamma_a \neq 0$). In both cases, we shall distinguish different parameter regimes. The behavior of the critical parameters with varying Pr and the eigenfunctions in the different regimes will also be presented.

A. Case of $\gamma_a = 0$

The case of zero thermal expansion parameter ($\gamma_a = 0$) corresponds to situations where the centrifugal buoyancy is small compared to the thermoelectric force. This assumption is reasonable for fluids with a small ratio $\gamma_a/\gamma_e = \alpha/e$ so that the results will be relevant to polar liquids with large coefficient e such as the acetonitrile and the nitrobenzene (Table I).

For a given working fluid (i.e., a fixed value of Pr) in a given annulus (i.e., a fixed value of η), the critical parameters are determined by varying the electric Rayleigh number L (i.e., varying the electric tension applied to the electrodes) as shown in Fig. 2. The temperature difference is fixed through the thermoelectric parameter γ_e. This is set at $\gamma_e = 0.01$ for outward heating where $L > 0$ and at $\gamma_e = -0.01$ for inward heating where $L < 0$. Yoshikawa *et al.* [21] has shown that, for annulus with $\eta < 0.9$, the critical parameters are insensitive to γ_e as far as $\gamma_e \leqslant 0.01$.

When there is no applied electric field ($L = 0$), the eigenvalue problem, Eqs. (16)–(21), reduces to that of the isothermal Taylor-Couette flow. The critical mode is steady axisymmetric ($\omega_c = 0$, $n_c = 0$). The known critical wavenumber $q_c = q_c^{\text{isoth}}$ and the known critical Taylor number $\text{Ta}_c = \text{Ta}_c^{\text{isoth}}$ [37] are recovered. When there is no rotation, i.e., when Ta = 0, the eigenvalue problem, Eqs. (16)–(21), reduces to the problem of the stability of a stationary conductive state under the DEP force. In the centripetal electric gravity, the heating should be outward for instability [21] so that our system can reach the critical condition only at a positive L for Ta = 0 [Fig. 2(a)].

For inward heating ($L < 0$), the critical Taylor number decreases with increasing L [Fig. 2(a)]. Under strong electric fields (i.e., large negative L), the critical mode is oscillatory axisymmetric (*Regime I*). The critical wavenumber varies slightly [Fig. 2(b)]. The frequency $|\omega_c|$ decreases with L and behaves as $|\omega_c| \propto |L|^{-1/2}$ at large $|L|$ [Fig. 2(c)]. Above a value $L = L^-$, the critical mode becomes stationary and the wavenumber jumps to a larger value around $q_c^{\text{isoth.}}$ [Fig. 2(b)]. This stationary axisymmetric mode is found for weak electric fields ($L \in [L^-,\ L^+]$) for both inward and outward heating (*Regime II*).

When the Taylor number is smaller than Ta^+, the electric Rayleigh number decreases with decreasing Ta and converges to the value for stationary electrodes [Fig. 2(a)]. The critical mode is nonaxisymmetric and oscillatory (*Regime III*), its frequency decreases and vanishes for stationary cylinders (Ta = 0). The critical mode number n_c increases with decreasing Ta. Discontinuities found in the behavior of q_c and ω_c reflects changes in n_c [Figs. 2(b) and 2(c)].

The parameter sets (L^-, Ta^-) and (L^+, Ta^+) which separate states of different stability nature are called *codimension-2 points*. At the point (L^-, Ta^-), both oscillatory and steady axisymmetric modes are critical; at the point (L^+, Ta^+), both steady axisymmetric and oscillatory nonaxisymmetric modes are critical. The values of L^- and Ta^- decrease with η; the value of L^+ increases with η, while Ta^+ approaches zero. Between these codimension-2 points, i.e., in Regime II, the critical mode consists of a steady axisymmetric vortex pattern with a wavenumber close to its value of isothermal Taylor vortices $q_c^{\text{isoth.}}$. Thermoelectric effects are not strong enough to change the nature of the Taylor instability, even though the critical Taylor number becomes much smaller than its isothermal value at large L. In the instability in Regime III, the

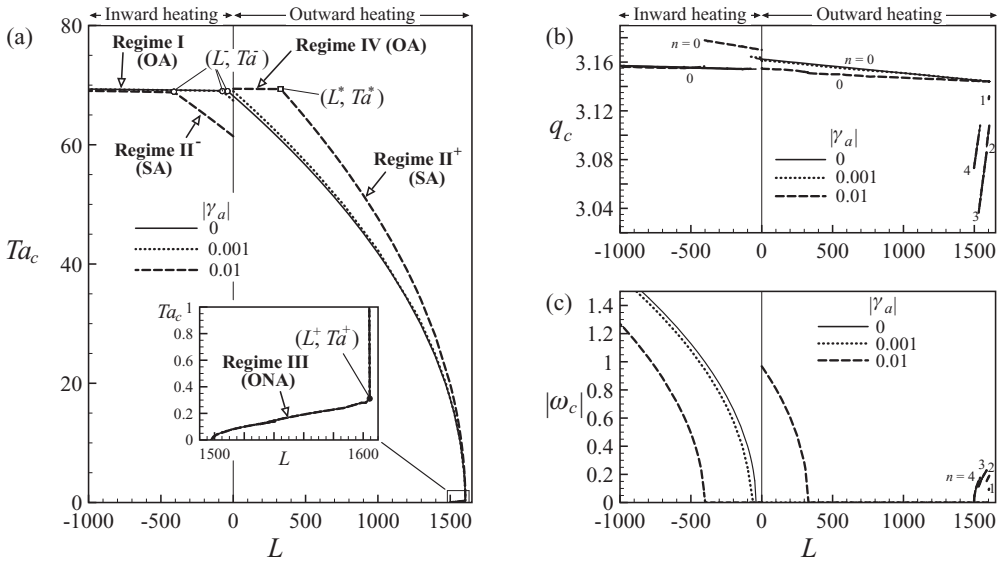

FIG. 3. Critical parameters for different thermal expansion parameters γ_a (Pr = 60, $\eta = 0.5$): Taylor number (a), wavenumber of vortices (b), and frequency (c). The thermoelectric parameter is fixed at $\gamma_e = -0.01$ and 0.01 for inward and outward heating, respectively. The critical modes are oscillatory axisymmetric (OA), steady axisymmetric (SA), or oscillatory nonaxisymmetric (ONA).

nonaxisymmetry of the thermoelectric critical mode at Ta = 0 is conserved, while the critical mode is oscillatory.

B. General case ($\gamma_a \neq 0$)

The critical parameters depend on the thermal expansion parameter γ_a, in particular under weak electric field (i.e., at small $|L|$). At $L = 0$ the behavior of the critical parameters becomes discontinuous (Fig. 3). Indeed, passing through zero from negative to positive L, we change the imposed temperature difference ΔT from a finite negative value to a finite positive value. As the centrifugal buoyancy breaks the symmetry of the stability of the Taylor-Couette flow with respect to the heating direction [14], we observe these discontinuities which are absent when $\gamma_a = 0$.

In inward heating, the qualitative behavior of the critical parameters are the same as in the case of $\gamma_a = 0$. The critical mode is oscillatory axisymmetric when $L < L^-$ (Regime I) and steady axisymmetric when $L \in [L^-, 0]$. We will refer to the latter regime as *Regime* II$^-$, because the critical modes have the same nature as those in Regime II. In Regime II$^-$ the critical Taylor number is lower than in the case of $\gamma_a = 0$. The codimension-2 point (L^-,Ta$^-$) separating Regimes I and II$^-$ shifts leftward [Fig. 3(a)] when the thermal expansion parameter becomes important.

In outward heating, a new regime (*Regime IV*) is observed for weak electric fields ($L \in [0, L^*]$) and large values of thermal expansion parameter γ_a (e.g., the case of $\gamma_a = 0.01$ in Fig. 3). The critical mode is oscillatory axisymmetric. Regime IV does not exist when γ_a is small (e.g., the case of $\gamma_a = 0.001$ in Fig. 3). The critical mode becomes steady axisymmetric (*Regime* II$^+$) beyond a new codimension-2 point (L^*,Ta*), recovering its nature in Regime II. Further increase of L results in the transition from the steady axisymmetric to oscillatory nonaxisymmetric critical modes (Regime III) at the codimension-2 point (L^+,Ta$^+$) as in the case of $\gamma_a = 0$.

C. Effects of the Prandtl number Pr

For stationary electrodes, the critical modes are steady and the Prandtl number has no influence on the critical parameters [21]. This independence can be confirmed by scaling the time by thermal diffusion time d^2/κ, the velocity by κ/d, and the generalized pressure by $\kappa\nu/d^2$. The resulting governing equations do not involve the Prandtl number for steady modes.

In the case of $\gamma_a = 0$, the similar argument leads to the independence of the critical parameters from Pr as long as the critical modes are steady axisymmetric. Therefore, the Prandtl number has no influence on critical values of the Taylor number Ta and the wavenumber q in Regime II. When the critical mode is oscillatory, the critical parameters vary with Pr. In Regime I, the critical Taylor number decreases significantly when the Prandtl number Pr is increased [Fig. 4(a)]. We found that the codimension-2 points, (L^-,Ta$^-$) and (L^+,Ta$^+$), are affected by Pr. The value of L^- increases significantly and is inversely proportional to Pr at large Pr: $L^- \propto -1/\mathrm{Pr}$ [Fig. 4(b)].

In the case of $\gamma_a \neq 0$, the critical values of the Taylor number depends on Pr even for steady axisymmetric modes. In inward heating, the critical Taylor number decreases both in Regime I and in Regime II$^-$ with increasing Pr [Fig. 4(a)]. The coordinate L^- separating these two regimes is smaller than in the case of $\gamma_a = 0$ [Fig. 4(b)]. It increases with the Prandtl number at small Pr, reaches a maximum value, and then decreases for large values of Pr. In outward heating, the critical Taylor number in Regime II$^+$ increases with the Prandtl number [Fig. 4(c)]. In contrast, it is insensitive to Pr in Regime IV, when this regime exists. In fact, there exists a minimum value of $\mathrm{Pr}_{\min}$ below which Regime IV does not exist. The coordinate L^* of the codimension-2 point between Regime IV and Regime II$^+$ vanishes at $\mathrm{Pr}_{\min}$ and increases for $\mathrm{Pr} > \mathrm{Pr}_{\min}$. The value of $\mathrm{Pr}_{\min}$ depends on the radius ratio η as well as on the thermal expansion parameter γ_a [Fig. 4(d)]. The electric Rayleigh number L^+ of the codimension-2 point between Regime II$^+$ and Regime III is not sensitive to the

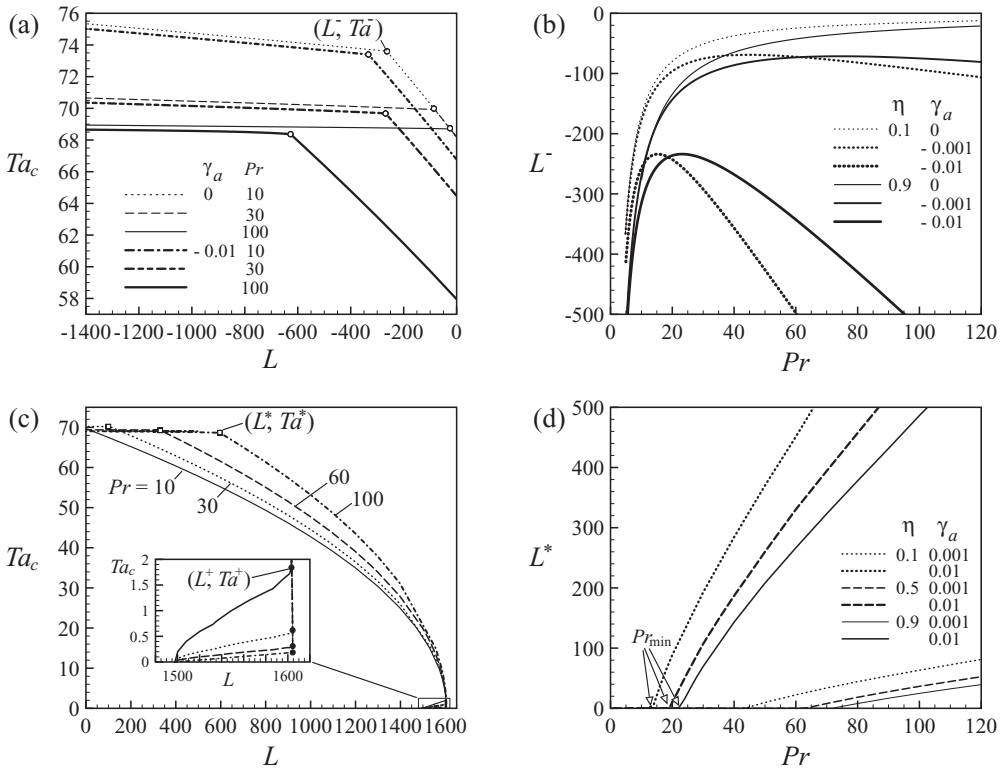

FIG. 4. Influence of the Prandtl number Pr on the critical parameters: (a) critical Taylor number ($\eta = 0.5$), (b) electric Rayleigh number at the codimension-2 point (L^-,Ta^-), (c) critical Taylor number ($\eta = 0.5$, $\gamma_a = 0.01$), and (d) electric Rayleigh number at the codimension-2 point (L^*,Ta^*). For all the results [(a)–(d)], the thermoelectric parameter is set at $\gamma_e = -0.01$ for inward heating and at $\gamma_e = 0.01$ for outward heating.

variation of Pr, while Ta^+ approaches zero with increasing Pr [Fig. 4(c)].

D. Eigenfunctions

The eigenfunctions of different states are illustrated in Fig. 5 (first column). The vortices of the critical modes are centered in the gap for large values of η, while they are shifted inward when η is small. The phase of the temperature perturbation θ' relative to the velocity field behaves differently in different regimes. In steady regimes, the phase is locked: in Regime II^-, the temperature θ' is in the antiphase of the radial velocity u'; in Regime II^+, they are in phase with each other. This means that in these regimes the flow goes from hot to cold walls inside the positive perturbation temperature zones, similar to the ordinary thermal convection. In the oscillatory regimes, the phase varies with the Rayleigh number L. In Regime I, the temperature advances (delays) to u' for positive- (negative-) ω_c modes by a phase difference larger than 90°. The phase difference increases with L and reaches 180° at the coodimension-2 point (L^-,Ta^-). In Regime IV, the phase difference is smaller than 90°. It decreases with L and becomes zero at the codimension-2 point (L^*,Ta^*).

V. DISCUSSION

In order to get a better understanding of the roles played by different forces in the flow stability, we have examined relative importance of the corresponding processes in the energy transfer from the base to perturbation states. We have also analyzed the frequencies of the oscillatory critical modes, inferring their scales from possible origins of the oscillation. We will make some comments on the flow stability under a centrifugal electric gravity field and the stability when the electric gravity changes its direction inside the gap.

A. Energy analysis

An evolution equation that governs the density of kinetic energy of the perturbation flow can be derived from the linearized Navier-Stokes Eqs. (17)–(19) by multiplying them by u', v', and w', respectively, and adding the results. After integrating over the whole gap, averaging over a wavelength and, for oscillatory modes, averaging over an oscillation period, one will find the following equation:

$$2\sigma K = W_{\mathrm{Ta}} + W_C + W_{\mathrm{BG}} + W_{\mathrm{PG}} - D_v, \qquad (24)$$

where K is the kinetic energy of the perturbation. The term W_{Ta} is the power performed by the centrifugal force, which is responsible for the Taylor instability, and the term W_C is the power input by the centrifugal buoyancy. The powers W_{BG} and W_{PG} represent the inputs from the thermoelectric buoyancies associated with the basic electric gravity $\boldsymbol{G}_e$ and the perturbation electric gravity $\boldsymbol{g}'_e$, respectively. The last term D_v is the viscous energy dissipation rate. At instability thresholds ($\sigma = 0$), it balances completely the sum of the other power terms.

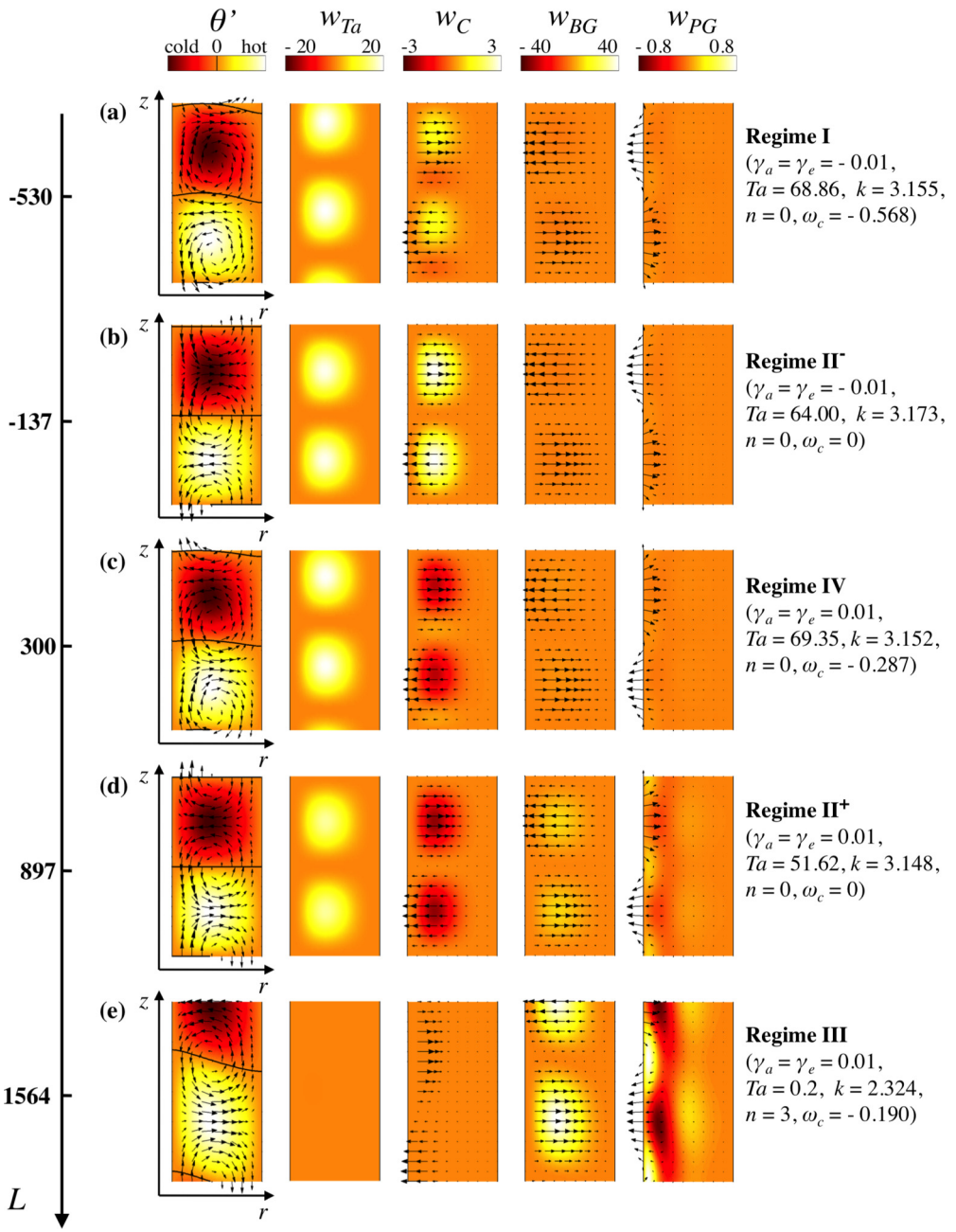

FIG. 5. (Color online) Eigenfunctions at critical conditions in different regimes ($\eta = 0.5$, $\mathrm{Pr} = 60$). The first, second, third, fourth, and fifth columns represent, respectively, (1) perturbation velocity (arrows) and perturbation temperature; (2) the local power w_{Ta}; (3) buoyancy associated with the centrifugal gravity (arrow) and w_C; (4) buoyancy associated with the base electric gravity $\boldsymbol{G}_e$ (arrows) and the power w_{BG}; (5) buoyancy due to the perturbation electric gravity $\boldsymbol{g}'_e$ (arrow) and the power w_{PG}. The powers are normalized by twice of the kinetic energy K. In the first column, temperature fields are shown without any numerical scale, as they are perturbation fields determined by a linear theory. Black curves are the contours of $\theta' = 0$. The values of electric Rayleigh number L used for computation are indicated on the L axis.

Each term in Eq.(24) is obtained from corresponding local and instantaneous power:

$$K = \langle \mathcal{K} \rangle = \left\langle \frac{|\boldsymbol{u}|'^2}{2} \right\rangle, \tag{25}$$

$$W_{\mathrm{Ta}} = \langle w_{\mathrm{Ta}} \rangle = \left\langle -u'v' \left(DV - \frac{V}{r} \right) \right\rangle, \tag{26}$$

$$W_C = \langle w_C \rangle = \left\langle -\frac{\gamma_a u' V}{r} \left(\theta' V + 2\Theta v' \right) \right\rangle, \tag{27}$$

$$W_{\mathrm{BG}} = \langle w_{\mathrm{BG}} \rangle = \left\langle \frac{L}{\mathrm{Pr}} \theta' G_e u' \right\rangle, \tag{28}$$

$$W_{\mathrm{PG}} = \langle w_{\mathrm{PG}} \rangle = \left\langle -\frac{L}{\mathrm{Pr}} \Theta \boldsymbol{g}'_e \cdot \boldsymbol{u}' \right\rangle, \tag{29}$$

$$D_v = \langle d_v \rangle = \langle 2\mathbf{e} : \mathbf{e} \rangle. \tag{30}$$

The rate-of-strain tensor is designated by $\mathbf{e} = [\nabla \boldsymbol{u}' + (\nabla \boldsymbol{u}')^T]/2$. Angle brackets mean the integration and averaging operations.

The power w_{Ta} of the centrifugal force is positive (Fig. 5, second column). Since $DV - V/r < 0$, it implies that the radial and azimuthal perturbation velocities, u' and v', are in phase with each other. The maxima of w_{Ta} are located at the points where the magnitude of the radial velocity is maximum. The power w_C of the centrifugal buoyancy depends on the phase of the temperature perturbation with respect to u', as well as on the heating direction (Fig. 5, third column). In total, it has positive and negative effects in inward and outward heating, respectively. The base electric gravity, in contrast, inputs net negative and positive power for inward and outward heating, respectively (Fig. 5, fourth column), as the electric gravity is opposed to the centrifugal acceleration. The power w_{PG} of the perturbation electric gravity is small compared to other energy transfer terms. It is concentrated in an inner region, while it almost vanishes in the outer region of the gap.

Figure 6 shows the behaviors of different terms in Eq.(24). In all the regimes except in Regime III, the power W_{Ta} is the main contribution to the energy transfer from the base state to perturbations. As inferred from local power inputs (Fig. 5), the power W_C by the centrifugal buoyancy is positive and negative in inward and outward heating, respectively, and the power W_{BG} by the thermoelectric buoyancy has the opposite sign to W_C. In Regimes I and IV where the critical modes are oscillatory, the net transfer $W_C + W_{\mathrm{BG}}$ by these two thermal buoyancies is negative, while it is positive in steady regimes, i.e., Regimes II^- and II^+. Increasing L in outward heating, the power W_{BG} becomes the most effective energy transfer process even in Regime II^+ at large L and dominates completely other transfer processes in Regime III. The power W_{PG} is always negative as found in the case of stationary electrodes [21], confirming the stabilizing effect of the perturbation electric gravity. Its contribution remains smaller than W_{Ta} or W_{BG}.

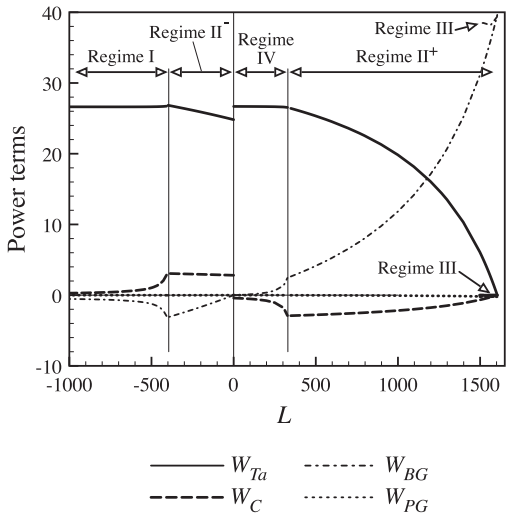

FIG. 6. Power terms in Eq. (24) normalized by twice of the kinetic energy K ($\eta = 0.5$, $\mathrm{Pr} = 60$; $\gamma_e = \gamma_a = 0.01$ for outward heating, $\gamma_e = \gamma_a = -0.01$ for inward heating).

B. Critical mode frequencies

According to the energetic analysis (Fig. 6), the thermoelectric buoyancy dominates other energy transfer processes in Regime III. On the other hand, the nonaxisymmetric nature of the critical modes obtained in the case of stationary electrodes persists in this regime. These observations suggest that the azimuthal base flow transports nonaxisymmetric perturbations amplified by the thermoelectric buoyancy to induce the critical mode oscillation. Indeed, the azimuthal phase velocity $c_\phi = -\omega_c/n_c$ of the perturbations is proportional to the Taylor number [Fig. 7(a)]. The constant of the proportionality depends on the radius ratio, but it does not depend on the Prandtl number.

In inward heating ($L < 0$), the centripetal electric gravity is directed from outer hot fluid zone to inner cold one. Thermoelectric buoyancy has then a stabilizing effect: it tends to bring back a deviated fluid parcel to its equilibrium radial position in the base state. In outward heating, the centrifugal acceleration is directed from hot to cold fluid zones so that the centrifugal buoyancy is stabilizing. As mentioned in the previous section, the net contribution of these two buoyancies is negative in Regimes I and IV (Fig. 6). This implies that the resulting force from the thermal buoyancies acts as a restoring force and would bear a close relation with the critical oscillatory modes obtained in these regimes.

In fluid with a stable density stratification, the balance between the fluid inertia and a restoring force results in wave propagation. For an oscillatory motion of a fluid parcel with a frequency N and with a small displacement ζ, its inertia per unit volume is estimated by $\rho N^2 \zeta$. The restoring force due to the radial thermal buoyancy is given by $-[d\rho(\Theta)/dr](G_e - G_c)\zeta$, where G_c is the centrifugal acceleration of the base flow: $G_c = V^2/r$. The sound speed has been assumed large enough to neglect the density variation associated with an isentropic process [38]. The balance between the inertial and restoring effects yields $N^2 = (-G_e + G_c)\, d(\log \rho)/dr$. This is a generalized Brunt-Väisälä frequency, which includes the effects of both the thermoelectric and centrifugal buoyancies. We can cast this frequency into the following dimensionless form by scaling it by the viscous time τ_v:

$$N = \sqrt{\frac{2(1-\eta)}{(1+\eta)\log\eta}\left[\frac{L}{\mathrm{Pr}} - \frac{\eta^3(3+\eta)^2}{2(1+\eta)^5}\gamma_a \mathrm{Ta}^2\right]}, \tag{31}$$

where G_e and G_c have been estimated at the midgap of the annulus. The right-hand side gives a real value only when the sum of the terms in the square brackets is negative: i.e., for inward heating, when the thermoelectric buoyancy dominates over the centrifugal one; for outward heating, when the centrifugal buoyancy is the dominant force. We have plotted the critical frequency ω_c as a function of N for different values of Pr and γ_a for Regimes I and IV[Fig. 7(b)]. When the critical frequency ω_c becomes larger than the unity, i.e., when the viscous dissipation is not significant during an oscillation period, the critical frequency is given by $\omega_c = N/3$ for $\eta = 0.9$. The factor of proportionality increases slightly

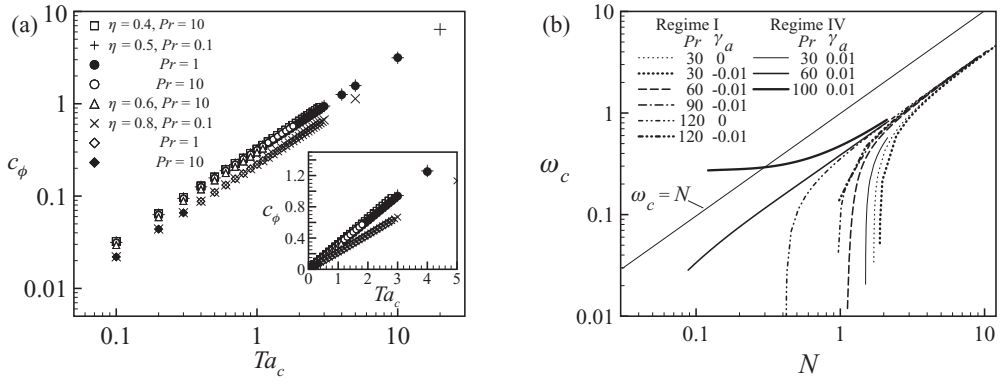

FIG. 7. Frequencies of the oscillatory critical modes obtained in Regimes I, III, IV: (a) phase velocity $c_\phi = -\omega_c/n_c$ in Regime III ($\gamma_e = 0.01$, $\gamma_a = 0$) and (b) frequency ω_c in Regimes I and IV ($\eta = 0.9$; $\gamma_e = -0.01$ in Regime I, $\gamma_e = 0.01$ in Regime IV).

with the radius ratio η, but it is insensitive to the Prandtl number. These observations suggest that oscillatory modes become critical in Regimes I and IV by receiving energy from the base flow through a resonant mechanism.

C. Stability in other gravity configurations

We have found for centripetal electric gravity fields that the behavior of the critical mode is closely related to the nature of the thermoelectric and centrifugal buoyancies. This is also the case when the electric gravity is centrifugal, i.e., when $G_e < 0$. As this configuration can occur only in inward heating ($\gamma_e < 0$), the accelerations $\boldsymbol{G}_e$ and $\boldsymbol{G}_c$ are both directed from cold to hot fluid zones. The associated thermal buoyancies are both destabilizing. The critical mode is hence steady, except when the azimuthal base flow transports nonaxisymmetric modes amplified by the thermoelectric instability.

In Fig. 8, the critical parameters and different power terms in Eq. (24) are shown for centrifugal electric gravity fields. The electric Rayleigh number defined by Eq. (4) takes positive values, as both γ_e and G_e are negative. With increasing the electric field, the critical Taylor number decreases and the critical wavenumber increases [Fig. 8(a)]. The power W_{Ta} performed by the centrifugal force remains the dominant energy transfer term until the Rayleigh number L approaches its critical value for stationary electrodes [Fig. 8(b)]. In the latter situation, the power W_{BG} due to the basic electric gravity is dominant so that the instability is thermoelectric one. The centrifugal electric gravity occurs only at large η [21], e.g., η should be larger than 0.99 for $\gamma_e = -0.01$. The mode degeneration observed in stationary annuli of large η [21] occurs in this thermoelectric regime. Nonaxisymmetric modes, which oscillate due to the base flow transport, as well as a steady axisymmetric mode are then both critical. The stabilizing effect of the perturbation electric gravity is also found to be important in the thermoelectric regime, as in Ref. [21]. This effect is more significant on small wavenumber modes and yields large critical wavenumbers at large L.

In inward heating, the electric gravity changes its direction within the gap when $\log\eta/(1+\log\eta) < \gamma_e < \log\eta$. The base electric gravity is centrifugal in an outer sublayer of the fluid, where the gravity is directed from cold to hot fluid zones and destabilizing. However, the base electric gravity is much smaller than the stabilizing perturbation electric gravity. In fact, the stability analysis for stationary electrodes [21] showed that the electric field cannot provoke any instability in this electric gravity configuration. The thermoelectric buoyancy has a net stabilizing effect and oscillatory modes can be critical. Indeed, the critical modes have nonzero frequency when the electric field is strong [Fig. 9(a)]. In this oscillatory regime, energy transfer due to the electric gravity $\boldsymbol{g}'_e$ occurs in an inner fluid layer [Fig. 9(b)] and its stabilizing effect dominates the destabilizing centrifugal buoyancy. At small L the destabilizing effect of the centrifugal buoyancy is dominant and the critical mode is steady. The flow goes in the same direction as and opposite to the centrifugal acceleration $\boldsymbol{g}_c$ inside, respectively, the cold and hot cores of perturbation temperature field [Fig. 9(c)].

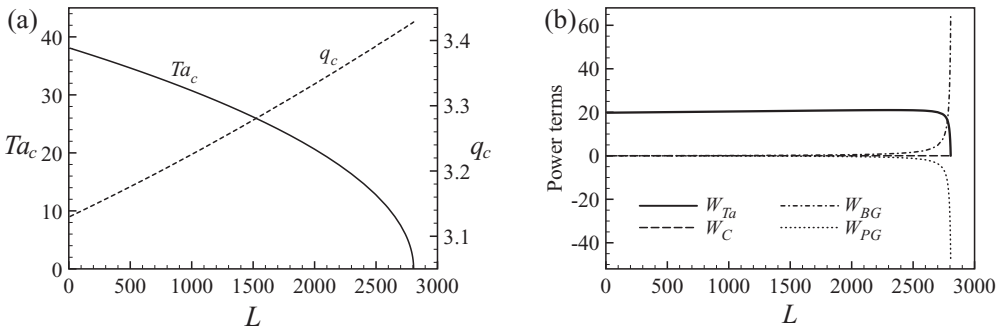

FIG. 8. Critical parameters (a) and power terms in Eq. (24) normalized by twice of the kinetic energy K (b), when the electric gravity $\boldsymbol{G}_e$ is centrifugal ($\eta = 0.995$, Pr $= 60$, $\gamma_a = \gamma_e = -0.01$).

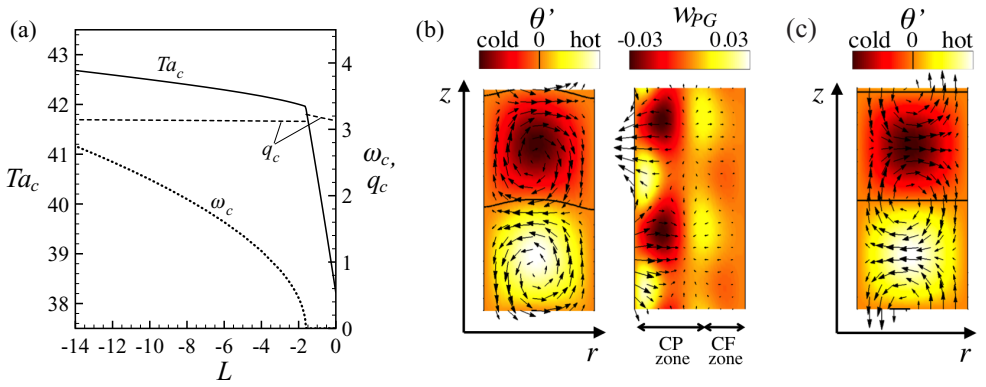

FIG. 9. (Color online) Critical parameters (a) and eigenfunctions (b, c) when the electric gravity $\boldsymbol{G}_e$ is centripetal (CP) in an inner layer and centrifugal (CF) in the outer layer ($\eta = 0.99009$, $\mathrm{Pr} = 60$, $\gamma_a = \gamma_e = -0.01$). In (b) where $L = -2.600$, the critical mode is oscillatory, while it is steady in (c) for $L = -1.200$. Arrows in the first image of (b) and in (c) show perturbation velocity fields. Arrows in the second image of (b) show the buoyancy field associated with the perturbation electric gravity $\boldsymbol{g}'_e$. The power w_{PG} is normalized by twice of the kinetic energy K. Temperature fields are shown without any numerical scale, as they are perturbation fields determined by a linear theory. Black curves are the contours of $\theta' = 0$.

For applications of the thermoelectric convection to heat exchangers, the present analysis should be extended to include the Earth's gravity. We are currently performing this extension for vertical Taylor-Couette systems. The resulting problem may have a lot of similarities to the thermomagnetic convection studied by Tagg and Weidman [15] under the Earth's gravity.

VI. CONCLUSION

A linear stability analysis has been performed for the Taylor-Couette flow of a dielectric fluid in the presence of a radial temperature gradient and a radial dielectrophoretic body force. The latter force arises from the thermal variation of the fluid electric permittivity and has been regarded as thermal buoyancy associated with an electric effective gravity. The critical parameters (the Taylor number Ta_c, the wavenumber q_c, and the frequency ω_c) have been determined for different values of the radius ratio, of the temperature difference and of the electric field strength. The thermal buoyancy due to the centrifugal acceleration is also taken into account in the analysis through the thermal expansion parameter γ_a. Different critical states have been identified. In inward heating, the critical mode is oscillatory axisymmetric (Regime I) and steady axisymmetric (Regime II^-) under strong and weak electric fields, respectively. Energy analysis showed that the centrifugal force is the dominant mechanism of energy transfer from the base state to perturbation flow in these regimes. In Regime I, thermal buoyancy has a net restoring effect, while it is destabilizing in Regime II^-. In outward heating, the critical mode is oscillatory axisymmetric (Regime IV), steady axisymmetric (Regime II^+), and oscillatory nonaxisymmetric (Regime III) in weak, moderate and strong electric fields, respectively. The dominant energy transfer mechanism is due to the centrifugal force in Regimes IV and II^+ and to the dielectrophoretic force in Regime III. Regime IV is found only when the thermal expansion parameter is significant, within certain ranges of the Prandtl number and radius ratio. The net contribution of the thermal buoyancy is stabilizing in Regime IV, while it is destabilizing in Regime II^+.

The frequencies of the oscillatory critical modes obtained in Regimes I and IV are correlated by the generalized Brunt-Väisälä frequency, which takes into account the restoring effects of the thermoelectric and centrifugal buoyancies. This finding indicates that in these oscillatory regimes, energy is transferred from the base flow to perturbation flow through a resonant mechanism. In Regime III, the critical nonaxisymmetric modes due to the thermoelectric buoyancy are advected by the azimuthal base flow. Their critical frequency is scaled by the frequency of the cylinder rotation.

ACKNOWLEDGMENTS

This work has been partly supported by the CNES (Centre National d'Etudes Spatiales) and the CNRS (Centre National de la Recherche Scientifique). Authors acknowledge the French National Research Agency (ANR) for financial support through the program *Investissements d'Avenir* (ANR-10-LABX-09-01), LABEX EMC3.

[1] C. D. Andereck, S. S. Liu, and H. L. Swinney, Flow regimes in a circular Couette system with independently rotating cylinders, J. Fluid Mech. **164**, 155 (1986).

[2] R. Ostilla-Mónico, E. P. van der Poel, R. Verzicco, S. Grossmann, and D. Lohse, Exploring the phase diagram of fully turbulent Taylor-Couette flow, J. Fluid Mech. **761**, 1 (2014).

[3] F. H. Busse, A model of mean zonal flows in the major planets, Geophs. Astrophys. Fluid Dynam. **23**, 153 (1983).

[4] A. R. Vasavada and A. P. Showman, Jovian atmospheric dynamics: An update after *Galileo* and *Cassini*, Rep. Prog. Phys. **68**, 1935 (2005).

[5] M. Lappa, *Rotating Thermal Flows in Natural and Industrial Processes* (Wiley, New York, 2012).
[6] H. A. Snyder and S. K. F. Karlsson, Experiments on the stability of Couette motion with a radial thermal gradient, Phys. Fluids **7**, 1696 (1964).
[7] M. M. Sorour and J. E. R. Coney, The effect of temperature gradient on the stability of flow between vertical, concentric, rotating cylinders, J. Mech. Engng Sci. **21**, 403 (1979).
[8] K. S. Ball, B. Farouk, and V. C. Dixit, An experimental study of heat transfer in a vertical annulus with a rotating inner cylinder, Int. J. Heat Mass Transfer **32**, 1517 (1989).
[9] V. Lepiller, A. Goharzadeh, A. Prigent, and I. Mutabazi, Weak temperature gradient effect on the stability of the circular Couette flow, Eur. Phys. J. B **61**, 445 (2008).
[10] K. G. Roesner, Hydrodynamic stability of cylindrical Couette-flow, Arch. Mech. **30**, 619 (1978).
[11] J.-C. Chen and J.-Y. Kuo, The linear stability of steady circular Couette flow with a small radial temperature gradient, Phys. Fluids A **2**, 1585 (1990).
[12] K. S. Ball and B. Farouk, Bifurcation phenomena in Taylor-Couette flow with buoyancy effects, J. Fluid Mech. **197**, 479 (1988).
[13] M. Ali and P. D. Weidman, On the stability of circular Couette flow with radial heating, J. Fluid Mech. **220**, 53 (1990).
[14] H. N. Yoshikawa, M. Nagata, and I. Mutabazi, Instability of the vertical annular flow with a radial heating and rotating inner cylinder, Phys. Fluids **25**, 114104 (2013).
[15] R. Tagg and P. D. Weidman, Linear stability of radially-heated circular Couette flow with simulated radial gravity, Z. Angew. Math. Phys. **58**, 431 (2007).
[16] P. J. Stiles, Electro-thermal convection in dielectric liquids, Chem. Phys. Lett. **179**, 311 (1991).
[17] L. D. Landau and E. M. Lifshitz, *Electrodynamics of Continuous Media*, 2nd ed., Landau and Lifshitz Course of Theoretical Physics, Vol. 8 (Butterworth-Heinemann, Oxford, 1984).
[18] J. R. Melcher, *Continuum Electromechanics* (The MIT Press, Cambridge, MA, 1981).
[19] P. H. Roberts, Electrohydrodynamic convection, Q. J. Mech. Appl. Math. **22**, 211 (1969).
[20] B. Chandra and D. E. Smylie, A laboratory model of thermal convection under a central force field, Geophys. Fluid Dynam. **3**, 211 (1972).
[21] H. N. Yoshikawa, O. Crumeyrolle, and I. Mutabazi, Dielectrophoretic force-driven thermal convection in annular geometry, Phys. Fluids **25**, 024106 (2013).
[22] B. Sitte and H. J. Rath, Influence of the dielectrophoretic force on thermal convection, Exp. Fluids **34**, 24 (2003).
[23] N. Dahley, B. Futterer, C. Egbers, O. Crumeyrolle, and I. Mutabazi, Parabolic flight experiment "Convection in a cylinder" - Convection patterns in varying buoyancy forces, J. Physics: Conference Series **318**, 082003 (2011).
[24] J. E. Hart, G. A. Glatzmaier, and J. Toomre, Space-laboratory and numerical simulations of thermal convection in a rotating hemispherical shell with radial gravity, J. Fluid Mech. **173**, 519 (1986).
[25] B. Futterer, M. Gellert, T. von Larcher, and C. Egbers, Thermal convection in rotating spherical shell: An experimental and numerical approach within GeoFlow, Acta Astronautica **62**, 300 (2008).
[26] B. Futterer, C. Egbers, N. Dahley, S. Koch, and L. Jehring, First identification of sub- and supercritical convection patterns from 'GeoFlow', the geophysical flow simulation experiment integrated in Fluid Science Laboratory, Acta Astronautica **66**, 193 (2010).
[27] B. Futterer, N. Dahley, S. Koch, N. Scurtu, and C. Egbers, From isoviscous convective experiment 'GeoFlow I' to temperature-dependent viscosity in 'GeoFlow II' - Fluid physics experiments on-board ISS for the capture of convection phenomena in Earth's outer core and mantle, Acta Astronautica **71**, 11 (2012).
[28] B. Futterer, A. Krebs, A.-C. Plesa, F. Zaussinger, R. Hollerbach, D. Breuer, and C. Egbers, Sheet-like and plume-like thermal flow in a spherical convection experiment performed under microgravity, J. Fluid Mech. **735**, 647 (2013).
[29] J. E. Hart and S. Kittelman, A magnetic fluid laboratory model of the global buoyancy and wind-driven ocean circulation: Experiments, Dyn. Atmos. Oceans **41**, 139 (2006).
[30] M. Takashima, Electrohydrodynamic instability in a dielectric fluid between two coaxial cylinders, Q. J. Mech. Appl. Math. **33**, 93 (1980).
[31] S. V. Malik, H. N. Yoshikawa, O. Crumeyrolle, and I. Mutabazi, Thermo-electro-hydrodynamic instabilities in a dielectric liquid under microgravity, Acta Astronautica **81**, 563 (2012).
[32] H. N. Yoshikawa, M. Tadie Fogaing, O. Crumeyrolle, and I. Mutabazi, Dielectric Rayleigh-Bénard convection under microgravity conditions, Phys. Rev. E **87**, 043003 (2013).
[33] P. J. Stiles and M. Kagan, Stability of cylindrical Couette flow of a radially polarised dielectric liquid in a radial temperature gradient, Physica A **197**, 583 (1993).
[34] R. J. Turnbull, Effect of dielectrophoretic forces on the Bénard instability, Phys. Fluids **12**, 1809 (1969).
[35] R. J. Turnbull and J. R. Melcher, Electrohydrodynamic Rayleigh-Taylor bulk instability, Phys. Fluids **12**, 1160 (1969).
[36] B. L. Smorodin and M. G. Velarde, On the parametric excitation of electrothermal instability in a dielectric liquid layer using an alternating electric field, J. Electrostatics **50**, 205 (2001).
[37] J. Walowit, S. Tsao, and R. C. DiPrima, Stability of flow between arbitrarily spaced concentric cylindrical surfaces including the effect of a radial temperature gradient, ASME J. Appl. Mech. **31**, 585 (1964).
[38] J. Lighthill, *Waves in Fluids* (Cambridge University Press, Cambridge, UK, 1978).